IOP Conf. Series: Journal of Physics: Conf. Series **1105** (2018) 012058 doi:10.1088/1742-6596/1105/1/012058

Lattice Boltzmann method in hydrodynamics and thermophysics

A L Kupershtokh[1] and D A Medvedev[2]

[1] National Research Novosibirsk State University, 2 Pirogova str., Novosibirsk, 630090, Russia
[2] Lavrentyev Institute of Hydrodynamics SB RAS, 15 Lavrentyev prosp., Novosibirsk, 630090, Russia

E-mail: skn@hydro.nsc.ru

Abstract. The variants of two- and three-dimensional lattice Boltzmann methods (LBM) are described for computer simulations of fluids with liquid-vapor phase transitions and heat transfer. Several improvements of LBM are described (correct implementation of the body force term, "pseudoforces" for the method of "passive scalar" for internal energy and implementation of a latent heat of evaporation). The formation of rivulets in a flow along an inclined flat surface, the fall of a droplet onto a rigid nonwettable plane and the process of spinodal decomposition of initially uniform fluid are modelled.

1. Introduction

In contrast to the classical methods of calculating fluid flows by solving the Navier–Stokes equations (CFD), the lattice Boltzmann equation method treats fluid flows as the motion of an ensemble of pseudoparticles on a regular lattice [1,2]. The main idea to use a discrete finite set of particle velocities $\mathbf{c}_k$ in the Boltzmann kinetic equation was proposed in [3].

Possible sets of velocity vectors $\mathbf{c}_k$ ($k = 0,1,...,b$) [4] for the two-dimensional nine-speed model D2Q9 on the square lattice ($b = 8$) and for the three-dimensional nineteen-speed model D3Q19 on the cubic lattice ($b = 18$) are shown in figures 1a and 1b. Moreover, during a time step Δt, all particles must move to neighboring lattice nodes ($\mathbf{e}_k = \mathbf{c}_k \Delta t$) [2, 3].

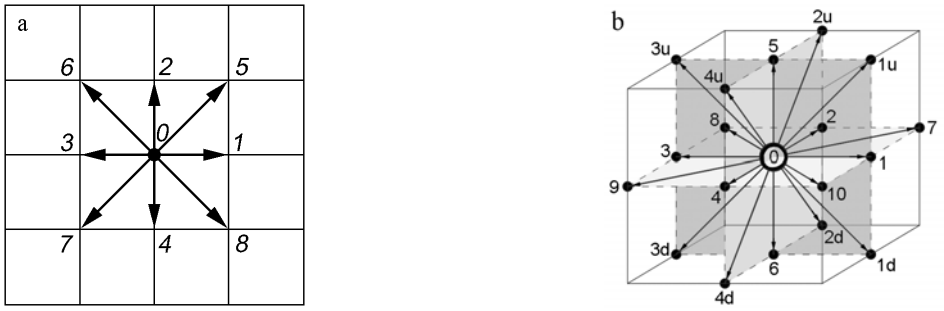

Figure 1. Possible sets of velocity vectors of pseudo particles in lattice Boltzmann method. Nine-speed model D2Q9 (a). Nineteen-speed model D3Q19 (b).

Actually, the algorithm of one-component two-phase lattice Boltzmann method includes the following steps:

- Preliminary choice of regular spatial lattice and corresponding pseudoparticle velocity set;
- Transfer of distribution functions (pseudoparticles) along the characteristics to the neighbor nodes;
- Implementation of a collision operator;
- Calculations of internal forces in accordance with a specific equations of state for fluids;
- Implementation of the total body forces acting on the fluid in nodes of lattice;
- Implementation of boundary conditions.

Hence, the evolution equation for the distribution functions $N_k(\mathbf{x},t)$ has the form

$$N_k(\mathbf{x}+\mathbf{c}_k\Delta t,t+\Delta t) = N_k(\mathbf{x},t)+\Omega_k(\{N\})+\Delta N_k\,, \tag{1}$$

where Δt is the time step, Ω_k is the collision operator, and ΔN_k is the change of the distribution functions due to the action of the external and internal body forces.

The density ρ and the velocity $\mathbf{u}$ of the fluid in a node can be calculated as

$$\rho = \sum\nolimits_{k=0}^{b} N_k\,, \tag{2}$$

$$\rho\mathbf{u} = \sum\nolimits_{k=1}^{b} \mathbf{c}_k N_k\,. \tag{3}$$

The collision operator with single relaxation time (BGK) can be used in the form

$$\Omega_k = (N_k^{eq}(\rho,\mathbf{u}) - N_k(\mathbf{x},t))/\tau\,, \tag{4}$$

where τ is the dimensionless relaxation time. This form of collision operator was proposed in [4,5] and simulates the tendency of the distribution functions to their equilibrium values

$$N_k^{eq}(\rho,\mathbf{u}) = \rho w_k\left(1+\frac{\mathbf{c}_k\mathbf{u}}{\theta}+\frac{(\mathbf{c}_k\mathbf{u})^2}{2\theta^2}-\frac{\mathbf{u}^2}{2\theta}\right). \tag{5}$$

Here, $\theta = (h/\Delta t)^2/3$ is the "kinetic" temperature of LBE pseudoparticles. In this case, the kinematic viscosity of fluid is equal to $\nu = \theta(\tau - 1/2)\Delta t$. The weight coefficients were calculated in [4] for the models D2Q9 and D3Q19.

The Exact Difference Method (EDM) was proposed in [6,7] to implement the body forces in the LBM. The change of distribution functions during the time step has the form

$$\Delta N_k(\mathbf{x},t) = N_k^{eq}(\rho,\mathbf{u}+\Delta\mathbf{u}) - N_k^{eq}(\rho,\mathbf{u})\,. \tag{6}$$

Here, $\mathbf{u}+\Delta\mathbf{u} = \mathbf{u}+\mathbf{F}\Delta t/\rho$ is the value of the velocity after the action of the total force $\mathbf{F}$ (internal forces and gravity) on a node. If the body forces are present, the physical value of fluid velocity is not equal to the velocity $\mathbf{u}$ used in LBM simulations, but should be recalculated at the half time step [8] as $\mathbf{u}_* = \mathbf{u}+\Delta\mathbf{u}/2$.

The justification for the LBE method is the fact that in the second order of the Chapman–Enskog expansion of the LBE equations, macroscopic equations of hydrodynamics (the continuity and Navier–Stokes equations) are obtained [9].

One can use the periodic boundary conditions, no-slip or slip boundary conditions on the solid surface and inflow/outflow boundary conditions. The well-known "bounce-back" rule is used for which the normal component of fluid velocity on a solid surface is zero.

2. Simulations of interphase boundaries between liquid and vapor

In order to simulate an attractive part of the intermolecular potential that ensures the condensation of vapor into liquid, it was proposed to introduce into LBM the forces of interaction between particles in neighbor nodes [10]. Later, the pseudopotential model was proposed in which the total force acting on the fluid in a node was introduced $\mathbf{F} = -\nabla U$ [11]. Here, the pseudopotential U can be defined using the equation of state for the fluid $U = P(\rho,T) - \rho\theta$.

The numerical approximation of the gradient of the pseudopotential is very important. In [12,13], the function $\Phi = \sqrt{-U}$ was specially introduced. Hence, we have $\mathbf{F} = 2A\nabla(\Phi^2) + (1-2A)2\Phi\nabla\Phi$. The corresponding finite-difference approximation of this formula was proposed in [12,13] as

$$\mathbf{F}(\mathbf{x}) = \frac{1}{\alpha h}\left[A\sum_k \frac{G_k}{G}\Phi^2(\mathbf{x}+\mathbf{e}_k)\mathbf{e}_k + (1-2A)\Phi(\mathbf{x})\sum_k \frac{G_k}{G}\Phi(\mathbf{x}+\mathbf{e}_k)\mathbf{e}_k \right]. \quad (7)$$

The constant α is equal to 3/2 and 3 for the models D2Q9 and D3Q19, respectively [13]. This so-called "combined" approximation is more stable than two approximations taken separately. The free parameter A can be tuned for each equation of state. Its optimal value is $A = -0.152$ for the van der Waals equation of state that can be written in the reduced variables $\widetilde{P} = P/P_{\text{cr}}$, $\widetilde{\rho} = \rho/\rho_{\text{cr}}$, $\widetilde{T} = T/T_{\text{cr}}$

$$\widetilde{P} = 8\widetilde{\rho}\widetilde{T}/(3-\widetilde{\rho}) - 3\widetilde{\rho}^2. \quad (8)$$

Here, $p_{\text{cr}}, \rho_{\text{cr}}, T_{\text{cr}}$ are the pressure, density and temperature at the critical point.

As a result, a phase boundary is represented as a thin transition layer between liquid and vapor where density changes smoothly over several lattice nodes (interface capturing). Moreover, the surface tension arises at interphase boundaries. The stability of LBM depends on the dimensionless parameter $\widetilde{k} = P_{\text{cr}}\Delta t^2/(\rho_{\text{cr}}h^2)$ [7]. The CUDA technology is used to parallelize the calculations on GPUs.

3. Simulation of wettability of a solid surface

Besides, the forces of interaction of fluid with the wettable solid surface should be also taken into account. The forces of interaction between the nodes that belong to the solid surface and the nodes that belong to the fluid determine the degree of wetting and, consequently, the values of contact angles. The simple model for the forces that acts on the fluid in the node $\mathbf{x}$ of fluid has the form [14]

$$\mathbf{F}_k(\mathbf{x}) = Bw_k\widetilde{\rho}(\mathbf{x})\widetilde{\rho}_{\text{eff}}(\mathbf{x}+\mathbf{e}_k)\,\mathbf{e}_k. \quad (9)$$

Here, $\widetilde{\rho}_{\text{eff}}$ is the effective reduced density of solid surface, B is the parameter of interaction. In fact, the wettability level and the values of the contact angles are determined only by the product $B\widetilde{\rho}_{\text{eff}}$.

4. Simulations of rivulets on inclined flat surface

The three-dimensional simulation of the rivulets flowing along an inclined flat surface in a gravity field (figure 2) is performed. No-slip boundary conditions are used at the solid surface. The periodic boundary conditions are used in y direction. The surface tension, evaporation, condensation, wettability of the surface and dynamic contact angles are taken into account.

The long heaters (figure 2a) ensure the prescribed temperature distribution on the surface in lateral direction $\widetilde{T}(y) = \widetilde{T}_0 + \Delta\widetilde{T}(1+\cos(2\pi y/\lambda))$ at $x > x_0$. Here, $\widetilde{T}_0 = 0.8$ is the reduced temperature of the surface without heaters, $\Delta\widetilde{T} = 0.06$. The wavelength is chosen so that $L_y = 3\lambda$. The reduced surface tension $\widetilde{\sigma} = \sigma/(P_{\text{cr}}h)$ depends on the temperature (figure 3). Hence, the ruptures of thin film in lateral direction can occur because of thermocapillary forces (Marangoni effect). Figures 2b and 2c show the evolution of the process during which a uniform flow of a thin liquid film is divided into

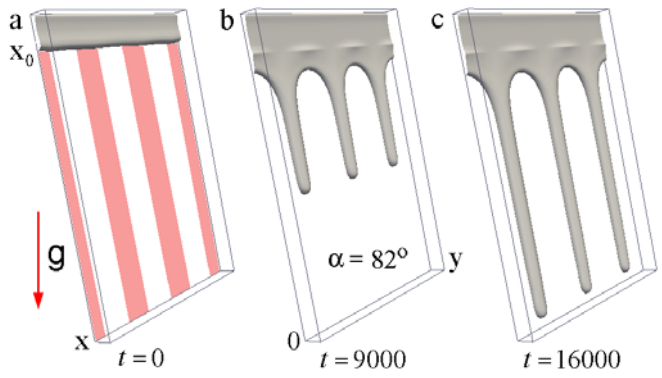

Figure 2. The flow of rivulets along an inclined flat solid surface in a gravity field. (a) The initial liquid film flow approaches to the leading edges of the heaters. (b-c) The development of rivulets. Lattice size is 1024×762×64.

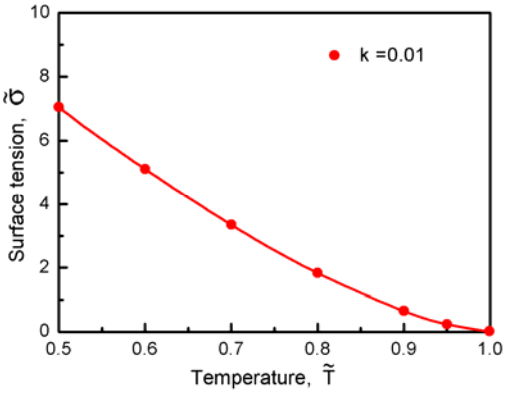

Figure 3. The temperature dependence of surface tension in the lattice Boltzmann method for van der Waals equation of state. $\tilde{k} = 0.01$.

three rivulets. Note, at the front edges of heaters, the small elevations are generated that are always observed in experiments (figures 2b and 2c).

5. Simulations of a droplet that falls onto a rigid flat plane

Three-dimensional simulations of the droplet that falls onto a horizontal flat nonwettable plane are carried out (figure 4). No-slip boundary conditions are used. The initial radius of the droplet is $\tilde{R} = 80$. The dimensionless surface tension at the temperature $\tilde{T} = 0.6$ is equal to $\tilde{\sigma} = 5.2$ at the dimensionless parameter $\tilde{k} = 0.01$ (see figure 3). The dimensionless gravity is $\tilde{g} = 7 \cdot 10^{-6}$.

After the droplet collides with the solid surface, the droplet initially spreads along the surface. The surface tension limits this process. After a while, the droplet takes a form close to the torus, and further expansion stops. Then, the surface tension tries to collect a liquid in a compact form. The shapes of the droplet at the spreading and receding stages are qualitatively similar to experimental ones [15]. However, on the axis, the cumulation of an axisymmetric convergent flow can occur. Occasionally at this moment in experiments with low-viscosity liquid, a vertical jet can be observed. Our simulations are performed on the lattice with relatively low resolution 640×640×224 ≈ 92000000 nodes and at the dimensionless kinematic viscosity $\nu = 0.023$ which is quite high. Consequently, we can observe only a moderate protrusion at the droplet surface. After several oscillations, the shape of the droplet takes the stable final form (figure 4f). The Bond and the Weber numbers in dimensionless variables are $\mathrm{Bo} = \tilde{\rho}\tilde{g}\tilde{R}^2/(\tilde{k}\tilde{\sigma})$ and $\mathrm{We} = \tilde{\rho}\tilde{R}\tilde{V}^2/(\tilde{k}\tilde{\sigma})$. Their values are $\mathrm{Bo} \approx 2$ and $\mathrm{We} \approx 3$.

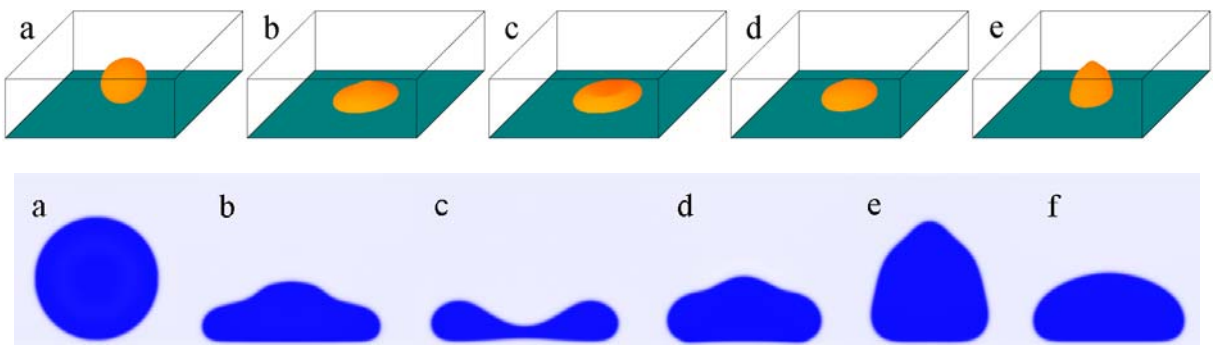

Figure 4. The droplet falls onto a rigid nonwettable plane. $t = 0$ (a); 2900 (b); 4500 (c); 6300 (d); 8300 (e); 29000 (f). Lattice size is 640×640×224.

6. Heat transfer in lattice Boltzmann method

The energy equation can be included in the LBE method in three main ways:

- by introducing an extended set of the particle velocities $\mathbf{c}_k$ [16] (the distribution functions depend also on the temperature $N_k^{eq}(\rho,\mathbf{u},T)$),
- by solving the equation for energy transfer in partial derivatives by one of the finite differences methods [17],
- by introducing an additional LBE component for the density of internal energy of fluid [18] (energy is considered as a passive scalar with zero mass that does not directly affect the momentum).

In the present work, we considerably improved the last method. The second set of distribution functions g_k is introduced which represents the density of internal energy $E = C_V T$ as $E = \sum g_k$. The evolution equation for g_k is

$$g_k(\mathbf{x}+\mathbf{c}_k\Delta t, t+\Delta t) = g_k(\mathbf{x},t) + \frac{g_k^{eq}(E,\mathbf{u}) - g_k(\mathbf{x},t)}{\tau_E} + g_k(\mathbf{x},t)\frac{\Delta E}{E} + \Delta g_k(\mathbf{x},t). \tag{10}$$

The second term in the right-hand side is the relaxation to the local equilibrium. The next term takes into account the change of the internal energy due to the heat conduction, the pressure work and the release or absorption of the latent heat of evaporation

$$\Delta E = \operatorname{div}(\lambda \operatorname{grad} T)\Delta t - P\operatorname{div}(\mathbf{u}_*)\Delta t - \frac{\rho_{liq}Q(T)}{\rho_2 - \rho_1}\rho\operatorname{div}(\mathbf{u}_*)\Delta t\,. \tag{11}$$

Here, $\rho_{liq}Q(T)$ is the latent heat per unit volume, ρ_1 and ρ_2 are some threshold values of density limiting the range in which the latent heat release is assumed, λ is the heat conductivity. The value of ΔE is calculated by finite differences. Other heat sources can also be included.

The last term in (10) $\Delta g_k(\mathbf{x},t)$ is the action of special "pseudoforces" that we introduce to prevent the parasitic spreading of energy at the phase boundaries. These "pseudoforces" are taken into account in the form similar to (6)

$$\Delta g_k(\mathbf{x},t) = g_k^{eq}(E,\mathbf{u}+\Delta\mathbf{u}) - g_k^{eq}(E,\mathbf{u}). \tag{12}$$

Two-dimensional simulations of a spinodal decomposition of the fluid are performed taking into account the pressure work and the evaporation latent heat. The initial distributions of the density and the temperature are uniform. The boundary conditions are periodic in x and y directions. The results are shown in figure 5. The temperature of expanding vapor initially decreases due to work of pressure (figure 5c). On the contrary, the temperature of liquid increases due to the release of latent heat (figure 5c). At the late stage, only two droplets surrounded by vapor remain. The saturated vapor pressure depends on the curvature of the surface. Hence, the pressure of vapor can not be saturated for both the smaller droplet and the larger one simultaneously. The results of simulation show that the smaller droplet has a lower temperature due to evaporation, and the larger one is heated because of condensation (figures 5b and 5d). This effect slows down the process of coarsening.

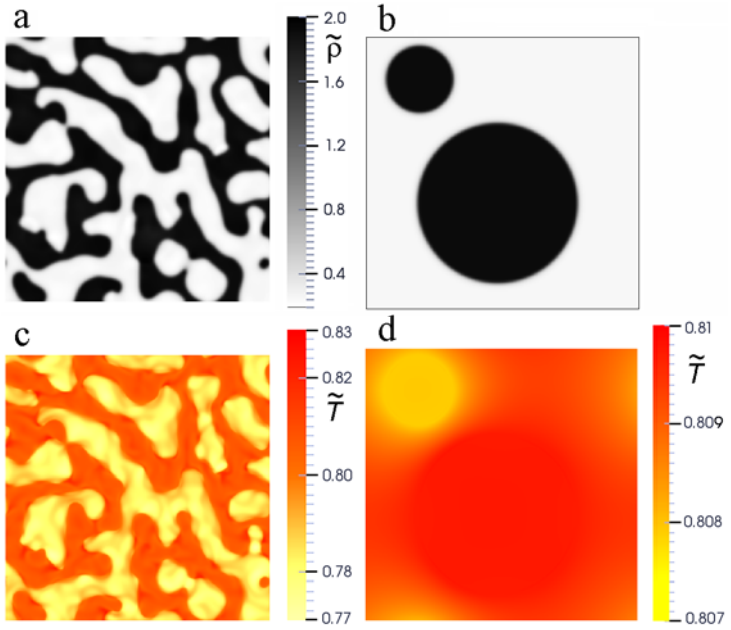

Figure 5. Distribution of density (a,b) and temperature (c,d). The initial stage $t = 2630$ (a,c) and the late stage $t = 1750000$ (b,d) of a spinodal decomposition of the fluid with initially uniform distributions of density and temperature ($\tilde{\rho}_0 = 1.0$, $\tilde{T}_0 = 0.8$). The grid size 500×500.

7. Conclusion

We have considerably improved the LBM. To include the heat transfer into the LBM, the special "pseudoforces" are added to the "passive scalar" approach for internal energy. The LBM is applied to several problems of hydrodynamics and thermophysics. The rupture of a liquid film flowing down along an inclined surface with local heating and the formation of rivulets are simulated. The impact of a droplet with a solid surface and the spinodal decomposition of the initially uniform state of the fluid are also simulated. To take into account the latent heat of phase transition, a new method is proposed.

Acknowledgments

The study was supported by the Russian Scientific Foundation (grant No. 18-19-10538).

References

[1] McNamara G R and Zanetti G 1988 Use of the Boltzmann equation to simulate lattice-gas automata *Phys. Rev. Lett.* **61**(20) 2332–5
[2] Higuera F J and Jiménez J 1989 Boltzmann approach to lattice gas simulations *Europhys. Lett.* **9**(7) 663–8
[3] Broadwell J E 1964 Study of rarefied shear flow by the discrete velocity method *J. Fluid Mech.* **19** 401–14
[4] Qian Y H, d'Humières D and Lallemand P 1992 Lattice BGK models for Navier–Stokes equation *Europhys. Lett.* **17**(6) 479–84
[5] Koelman J M V A 1991 A simple lattice Boltzmann scheme for Navier–Stokes fluid flow *Europhys. Lett.* **15**(6) 603–7
[6] Kupershtokh A L 2004 New method of incorporating a body force term into the lattice Boltzmann equation *Proc. 5th Int. EHD Workshop* (University of Poitiers, Poitiers, France) pp 241–6
[7] Kupershtokh A L 2010 Criterion of numerical instability of liquid state in LBE simulations *Computers and Mathematics with Applications* **59**(7) 2236–45
[8] Ginzburg I and Adler P M 1994 Boundary flow condition analysis for the three-dimensional lattice Boltzmann model *J. Phys. II France* **4**(2) 191–214
[9] Chen S and Doolen G D 1998 Lattice Boltzmann method for fluid flow *Annu. Rev. Fluid Mech.* **30** 329–64

[10] Shan X and Chen H 1993 Lattice Boltzmann model for simulating flows with multiple phases and components *Physical Review* E **47**(3) 1815–9
[11] Qian Y H and Chen S 1997 Finite size effect in lattice-BGK models *Int. J. Modern Physics* C **8**(4) 763–71
[12] Kupershtokh A L, Stamatelatos C and Agoris D P 2005 Stochastic model of partial discharge activity in liquid and solid dielectrics *Proc. IEEE 15th Int. Conf. on Dielectric Liquids* (University of Coimbra, Coimbra, Portugal) pp 135–8
[13] Kupershtokh A L, Medvedev D A and Karpov D I 2009 On equations of state in a lattice Boltzmann method *Computers and Mathematics with Applic*ations **58**(5) 965–74
[14] Kupershtokh A L, Ermanyuk E V and Gavrilov N V 2015 The rupture of thin liquid films placed on solid and liquid substrates in gravity body forces *Communications in Comp. Phys.* **17**(5) 1301–19
[15] Roisman I V, Rioboo R and Tropea C 2002 Normal impact of a liquid drop on a dry surface: model for spreading and receding *Proc. R. Soc. Lond.* A **458** 1411–30
[16] Alexander F J, Chen S and Sterling J D 1993 Lattice Boltzmann thermohydrodynamics *Phys. Rev.* E **47**(4) R2249–52
[17] Zhang R, Chen H 2003 Lattice Boltzmann method for simulations of liquid-vapor thermal flows *Phys. Rev.* E **67**(6) 066711
[18] He X, Chen S and Doolen G D 1998 A novel thermal model for the lattice Boltzmann method in incompressible limit *J. Comp. Phys.* **146**(2) 282–300